4

REPORT SSD-TR-90-19

Heat Loads Due to the Space Particle Environment

Prepared by

A. L. VAMPOLA and J. E. COX
Space Sciences Laboratory
Laboratory Operations

and

R. D. JIMENEZ
Architecture Planning and Technology Division
Development Group
The Aerospace Corporation
El Segundo, CA 90245-4691

6 August 1990

Prepared for

SPACE SYSTEMS DIVISION
AIR FORCE SYSTEMS COMMAND
Los Angeles Air Force Base
P.O. Box 92960
Los Angeles, CA 90009-2960

This report was submitted by The Aerospace Corporation, El Segundo, CA 90245, under Contract No. F04701-88-C-0089 with the Space Systems Division, P.O. Box 92960, Los Angeles, CA 90009-2960. It was reviewed and approved for The Aerospace Corporation by H. R. Rugge, Acting Director, Space Sciences Laboratory. Lt Fisher was the project officer for the Mission-Oriented Investigation and Experimentation (MOIE) Program.

This report has been reviewed by the Public Affairs Office (PAS) and is releasable to the National Technical Information Service (NTIS). At NTIS, it will be available to the general public, including foreign nationals.

This technical report has been reviewed and is approved for publication. Publication of this report does not constitute Air Force approval of the report's findings or conclusions. It is published only for the exchange and stimulation of ideas.

Tyron Fisher

TYRON FISHER, LT, USAF
MOIE Project Officer
SSD/CLPO

Raymond M. Leong

RAYMOND M. LEONG, MAJ, USAF
MOIE Project Manager
AFSTC/WCO OL-AB

UNCLASSIFIED

SECURITY CLASSIFICATION OF THIS PAGE

REPORT DOCUMENTATION PAGE

1a. REPORT SECURITY CLASSIFICATION Unclassified	1b. RESTRICTIVE MARKINGS
2a. SECURITY CLASSIFICATION AUTHORITY	3. DISTRIBUTION/AVAILABILITY OF REPORT Approved for public release; distribution unlimited.
2b. DECLASSIFICATION/DOWNGRADING SCHEDULE	
4. PERFORMING ORGANIZATION REPORT NUMBER(S) TR-0089(4940-06)-1	5. MONITORING ORGANIZATION REPORT NUMBER(S) SSD-TR-90-19
6a. NAME OF PERFORMING ORGANIZATION The Aerospace Corporation Laboratory Operations 6b. OFFICE SYMBOL (If applicable)	7a. NAME OF MONITORING ORGANIZATION Space Systems Division
6c. ADDRESS (City, State, and ZIP Code) El Segundo, CA 90245-4691	7b. ADDRESS (City, State, and ZIP Code) Los Angeles Air Force Base Los Angeles, CA 90009-2960
8a. NAME OF FUNDING/SPONSORING ORGANIZATION 8b. OFFICE SYMBOL (If applicable)	9. PROCUREMENT INSTRUMENT IDENTIFICATION NUMBER F04701-88-C-0089
8c. ADDRESS (City, State, and ZIP Code)	10. SOURCE OF FUNDING NUMBERS PROGRAM ELEMENT NO. / PROJECT NO. / TASK NO. / WORK UNIT ACCESSION NO.

11. TITLE (Include Security Classification)

Heat Loads Due to the Space Particle Environment

12. PERSONAL AUTHOR(S)

Vampola, A. L., Cox, J. E., and Jimenez, R. D.

13a. TYPE OF REPORT	13b. TIME COVERED	14. DATE OF REPORT (Year, Month, Day)	15. PAGE COUNT
	FROM ____ TO ____	1990 August 6	16

16. SUPPLEMENTARY NOTATION

17. COSATI CODES			18. SUBJECT TERMS (Continue on reverse if necessary and identify by block number)
FIELD	GROUP	SUB-GROUP	Space cryogenics Satellite heating Particle heating

19. ABSTRACT (Continue on reverse if necessary and identify by block number)

Analysis of the heat load imposed upon a satellite by the energetic particle population trapped in the magnetosphere indicates that this source of heat can provide as much as 0.5 W/M^2 for short periods. During times of magnetic storms, this value can further increase by half an order of magnitude. This heat source should be considered for any space system with elements designed to run below 100 K and becomes nonnegligible for systems with passively cooled elements (radiators) designed to run below 75 K. Below 60 K, this may be a major concern in the design of the thermal system. In general, the heating due to trapped energetic particles is small in low altitude orbits, moderate in geosynchronous orbits, and severe in intermediate orbits such as the GPS orbit. Average heating in high inclination orbits is lower than in low inclination orbits.

20. DISTRIBUTION/AVAILABILITY OF ABSTRACT ☒ UNCLASSIFIED/UNLIMITED ☐ SAME AS RPT. ☐ DTIC USERS	21. ABSTRACT SECURITY CLASSIFICATION Unclassified
22a. NAME OF RESPONSIBLE INDIVIDUAL	22b. TELEPHONE (Include Area Code) / 22c. OFFICE SYMBOL

DD FORM 1473, 84 MAR — 83 APR edition may be used until exhausted. All other editions are obsolete

SECURITY CLASSIFICATION OF THIS PAGE

UNCLASSIFIED

PREFACE

Portions of this work were supported by an Advanced Study Grant from The Aerospace Corporation and by the USAF System Command's Space System Division under Contract F04071-88-C-0089. Impetus for this analysis originated in a PhD dissertation (Ref. 1) by one of the authors, R. D. Jimenez.

A-1

CONTENTS

FIGURES

I. INTRODUCTION

While the total energy content of the energetic particles trapped in the earth's geomagnetic field is small, space systems which attempt to use super-cold elements, such as long-wavelength IR optics, must consider this source of heat input. In the most intense part of the radiation belts, the peak instantaneous heat input is equivalent to that which would be radiated by a black body at a temperature in excess of 55 K. This source of heat begins to have a measurable effect at a radiator temperature of about 100 K in some orbits. In these same orbits, at a radiator temperature of 60 K, the thermal analysis would have to include the effect of this heat source. At lower radiator temperatures, in the order of 50 K, this source of heat would become a major problem and would be a prime driver in the thermal design. Obviously, for very low temperature elements such as HgCdTe detectors, which are intended to be radiatively cooled either directly or through a secondary radiator, trapped particle heating will have to be included as part of the input load in the thermal analysis.

II. DISCUSSION

In this report, we present a table of average and peak heat inputs for a number of orbits. The table was generated using the NASA environments AP8MIN and AE8MAX. We include a plot of the heat input as a function of time for a 24 hr period to indicate the type of thermal profile one might expect in a particular orbit. We also discuss the accuracy of the heat calculations, the accuracy of the particle models, and the variability of the particle environment itself. The plots included in this report are intended only as a guide to the level of trapped particle heating that may occur in a particular orbit. The accuracy of the individual data points that are plotted or are listed in Table 1 is limited by the accuracy of the trapped particle models which were used to determine the particle fluxes for the various orbits. In general, the particle models are good to a factor of 2 or 3 for long-term averages. The calculations provide the total energy flux through a surface without regard to the depth in materials at which this energy will be deposited. However, the highest heating rate will occur at the surface. The heat due to the protons is deposited nearer the surface than that due to the electrons because the protons have a much higher linear energy transfer (LET) coefficient. In most orbits, 99% of the proton heat and 84% of the electron heat would be generated in a thin layer of aluminum 0.25 mm thick (Ref. 1).

A. MODEL ACCURACIES AND TRAPPED PARTICLE FLUX VARIATIONS

The calculations presented in this document used the NASA AP8 (Aerospace Proton #8) and AE8 (Aerospace Electron #8) models. These are the most recent updates to the models of the trapped radiation environments. The accuracy of the AP8 model is probably better than a factor of 2 in the inner zone (altitudes up to 3000 nm at low inclination). In the outer zone, the accuracy is somewhat less certain, but is again probably good to a factor of 2. Similarly, the AE8 model is probably accurate to a factor of 2 or better in the inner zone. In the outer zone, for long term averages (averaged over a solar cycle), the AE8 model is probably low by about a factor of 3 for electrons with energies above 1.5 MeV. However,

the major portion of the heat load due to trapped electrons is due to the particles with energies between 100 keV and 500 keV. Furthermore, in some orbits examined, protons contribute more heat input (~75%) than the electrons. For the purposes of analyzing heat input from trapped particles, electrons with energies above 500 keV can be ignored without affecting the accuracy of the estimates. Therefore, inaccuracies in the electron models are probably unimportant.

While the inaccuracies in the particle models may not be important, the variations in the electron flux due to magnetic storms are. Immediately after a major magnetic storm, the entire outer zone electron spectrum above about 100 keV is enhanced by a factor of 10 to several hundred. The lower energy electrons, below 100 keV, are more constant. It takes several weeks for this enhancement to subside (Ref. 2). For a satellite traversing this region of space, a significant increase in heating above normal would be observed.

Figure 1 is a plot of the 0.54 MeV electron flux at various L values showing the response of the particle distribution to a number of magnetic storms over an 11 month period (Ref. 2). The term "L value" used in this discussion refers to properties of the field lines. In a dipole field, the L value corresponds to the distance from the center of the dipole to the equatorial crossing of the field line, in units of earth radii. The field line retains its L value designation all along its length, including the extension to low altitudes at higher latitudes. Note that for some parts of the magnetosphere, magnetic storms create an electron flux enhancement of as much as 4 orders of magnitude. The models take these enhancements into consideration in determining average flux values. In general, for short times after major magnetic storms, the integral flux above 100 keV is enhanced by up to a factor of 10 over the average values. These enhancements will be particularly effective in increasing the transient heat load in orbits which traverse the outer zone between altitudes of 7000 and 12000 nm, where the most intense outer zone electron flux exists.

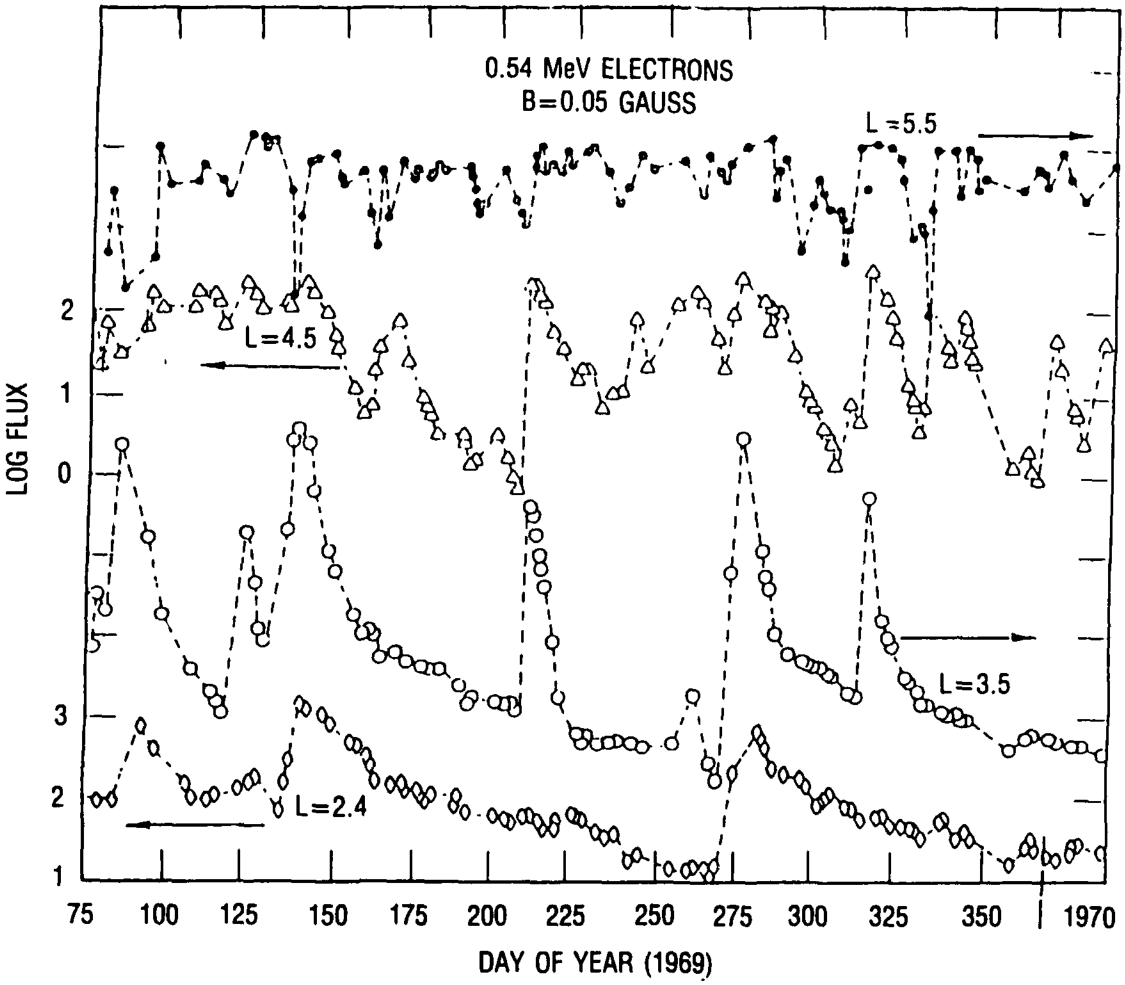

Figure 1. Response of Outer Zone Electrons to Magnetic Storms

Figure 2 is a plot of the integral electron number flux (dashed lines) and the proton flux (solid lines) as a function of time during a 24 hr orbit integration period in a low altitude, low inclination orbit. The peak fluxes observed here correspond to the peak heating levels listed in Table 1. Although a rigorous analysis of the instantaneous heating rate would include an integration of the flux energy spectra, the flux spectra do not change sufficiently over an orbit to invalidate direct use of these curves in comparing the average and peak values listed in Table 1. The error due to uncertainties in the models is greater than the error which results in assuming there is no variation in the energy spectrum. The strong modulation in the flux intensity is due to the passage of the orbit through the South Atlantic Anomaly region.

B. DISCUSSION OF TABLE 1

For this discussion, "peak" refers to the peak-heating-per-orbit, as depicted in Figure 2, not the peak that will be encountered due to magnetic storms during a long duration mission. For orbits which have outer zone electrons or protons as their major heat input, magnetic storms can increase the short period peak heating (1 to 2 days) over that listed in the table by a factor of 10. Major interpolations in orbital altitude using Table 1 should not be performed because the proton and electron environments are strong nonmonotonic functions of altitude. Interpolations on orbital inclination, however, will yield results which are reasonably valid.

1. 400 NM CIRCULAR ORBIT

The 400 nautical mile (NM) circular orbit encounters relatively little energetic particle flux. For low inclinations, the offset dipole of the earth's magnetic field effectively raises the trapped population above this altitude. Only in the region of the South Atlantic Anomaly, about 290° ± 20° east longitude, does the low latitude flux occur at low enough altitudes for significant heat input to be observed in this orbit. Thus, both the average and peak heat inputs are low. The entire heat input occurs during about a 25 min period out of each orbit. At 30° inclination,

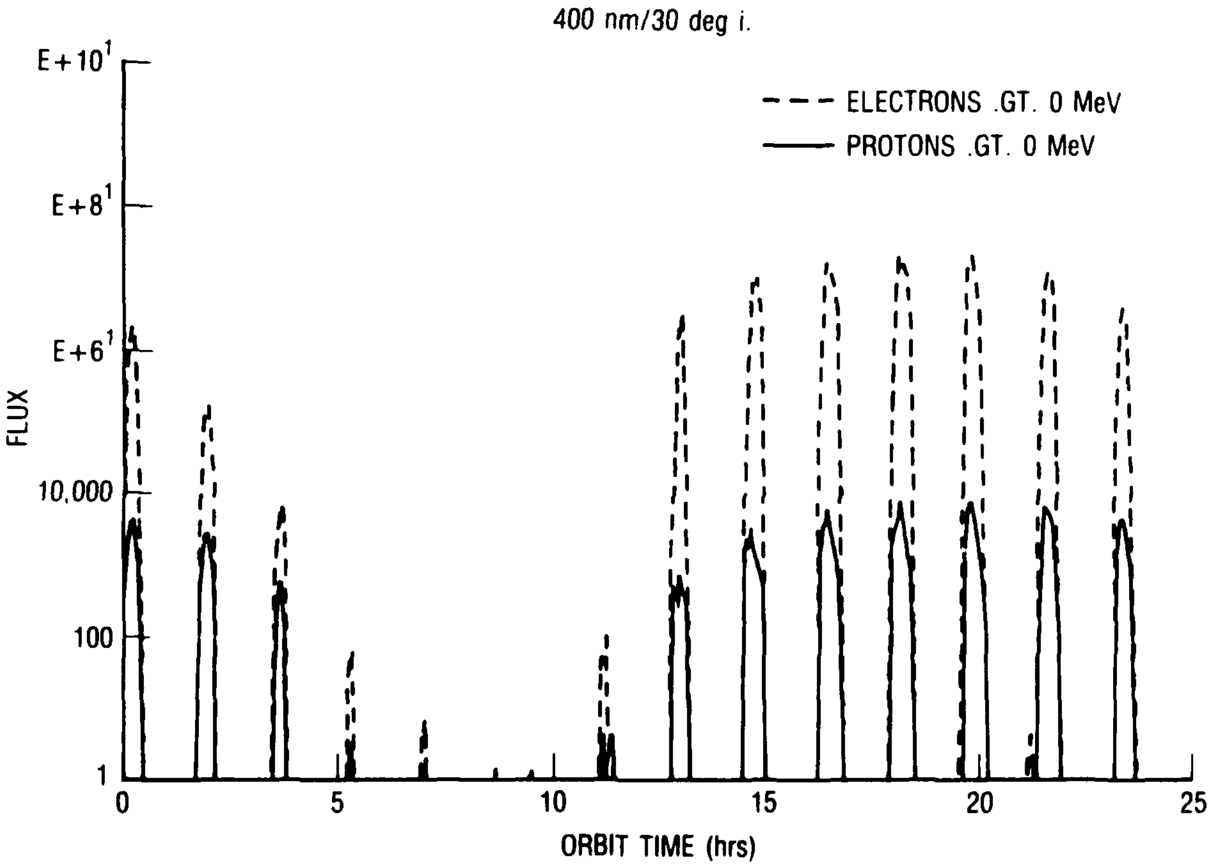

Figure 2. Heat Input vs Orbit Time

Table 1. Particle-Induced Satellite Heating (Watts/Meter^2)

Inclination	400 NM Circular		12 hr Elliptical		12 hr Circular		24 hr Circular	
	Avg	Peak	Avg	Peak	Avg	Peak	Avg	Peak
0°	9.0×10^{-6}	1.2×10^{-4}	8.7×10^{-2}	5.5×10^{-1}	1.4×10^{-1}	1.6×10^{-1}	1.3×10^{-2}	1.6×10^{-2}
30°	2.1×10^{-4}	5.3×10^{-3}	4.8×10^{-2}	4.8×10^{-1}	8.4×10^{-2}	1.6×10^{-1}	1.1×10^{-2}	3.1×10^{-2}
60°	2.4×10^{-4}	7.7×10^{-3}	2.2×10^{-2}	3.3×10^{-1}	4.3×10^{-2}	1.6×10^{-1}	5.7×10^{-3}	2.8×10^{-2}
90°	1.9×10^{-4}	8.1×10^{-3}	1.8×10^{-2}	3.2×10^{-1}	3.6×10^{-2}	1.6×10^{-1}	4.7×10^{-3}	2.8×10^{-2}

however, larger fluxes of energetic electrons and protons are encountered due to the orbit intersecting the low altitude extensions of the outer electron zone and the inner proton zone. Since the orbit cuts through this outer zone extension at an angle, the period during which the maximum heating occurs is spread over approximately 30 min. Magnetic storm-time increases in the outer zone electrons will increase the peak heat input by another order of magnitude over the values shown in the table. This is because the maximum in the table is due to the outer zone fluxes and these can increase by a factor of 10 over the average in the models.

At 60° and 90° inclinations, the orbit passes through the outer electron zone more rapidly, but it also samples more of the outer zone (all of it, in the case of the 90° orbit). Although the peak heating is highest for the 90° orbit, it occurs for shorter durations than for the 30° inclination; thus the average heat input is lower than for the 30° inclination.

2. 12 HR ELLIPTICAL ORBIT

For these calculations, the apogee was at the equator. This orbit, which at higher inclination is known as the "Molniya" orbit, is the most severe orbit from the point of view of instantaneous trapped particle heating. Average heating, however, is less than for the 12 hr circular orbit. (A 10 hr circular orbit would have even higher average heating, but the same peak heating.) In the 12 hr elliptical orbit, along with the high heat load, a high radiation dose effect is also present. Increasing the latitude of apogee will reduce the average heat input, but may increase the peak heat load. Both the peak and average heat loads decrease monotonically with increasing inclination. This is because the peak outer zone electron and proton fluxes occur well below apogee, and the higher the inclination of the orbit, the farther away from the equator this region is traversed. Since the flux generally decreases monotonically with increasing distance from the geomagnetic equator, the higher inclination orbits encounter less flux.

3. 12 HR CIRCULAR ORBIT

For the 12 hr circular orbit, the trapped particle heat load is due primarily to the 1 to 10 MeV protons in the outer zone. Protons constitute 80% of the average heat load at low inclination, and 70% at high inclinations. While major magnetic storms will increase the total heat load, an order of magnitude increase in electrons would increase the heat load by only a factor of 3. The average trapped particle heating is a strong function of inclination up to perhaps 45°. The peak heating rate is virtually independent of inclination because the peak heating occurs at the equator and all orbit inclinations pass through the geomagnetic equator at nearly the same L value.

4. 24 HR CIRCULAR ORBIT

In the geosynchronous region, proton energies are relatively low. At the same time, energetic electron fluxes are high and remain near the trapping limit (the maximum equilibrium flux the field line can sustain) most of the time. As a result, the electrons contribute most of the heating at 0° inclination. Magnetic storms are not important in this orbit because they do not cause major increases in the electron flux (see Figure 1). Also, at this altitude, the offset dipole of the earth's magnetic field does not produce any significant effects. However, the distortion of the magnetosphere due to the solar wind does produce local time variations. These local time effects are significant in the energetic electron flux, especially in the >500 keV range, and produce the difference between average and peak heating at 0° plus much of the variation seen in the peak heating as a function of inclination.

At geosynchronous orbit, the peak heating in high inclination orbits is due to protons even though the average heating is primarily due to electrons. This is caused by hot plasma conditions beyond L=6.6. In this high altitude regime, there are usually large fluxes of protons with energy in the tens of keV range, while few energetic electrons are present.

III. SUMMARY

The trapped particle population can produce significant heating in some systems. Model calculations indicate that greater than 0.5 W/M^2 instantaneous heat input may be encountered. For some orbits, geomagnetic storms can produce an increase in the energetic particle flux that results in a further increase in the average heat input by half an order of magnitude and an increase of an order of magnitude in the peak heat input. For very low temperature systems, the trapped particle heating may be the major heat source. For systems intended to operate at 100 K or colder with radiative cooling systems, this mechanism should be considered in the thermal analysis. Below 60 K, the heating due to trapped particles may be a major concern in the design of the system in some orbits.

In general, low altitude orbits are benign and orbits which pass through the heart of the outer zone (L=4 at the equator) are fairly severe. Geosynchronous orbits are in between these extremes. Also, the higher the inclination of the orbit, the lower the average heating.

LABORATORY OPERATIONS

The Aerospace Corporation functions as an "architect-engineer" for national security projects, specializing in advanced military space systems. Providing research support, the corporation's Laboratory Operations conducts experimental and theoretical investigations that focus on the application of scientific and technical advances to such systems. Vital to the success of these investigations is the technical staff's wide-ranging expertise and its ability to stay current with new developments. This expertise is enhanced by a research program aimed at dealing with the many problems associated with rapidly evolving space systems. Contributing their capabilities to the research effort are these individual laboratories:

Aerophysics Laboratory: Launch vehicle and reentry fluid mechanics, heat transfer and flight dynamics; chemical and electric propulsion, propellant chemistry, chemical dynamics, environmental chemistry, trace detection; spacecraft structural mechanics, contamination, thermal and structural control; high temperature thermomechanics, gas kinetics and radiation; cw and pulsed chemical and excimer laser development including chemical kinetics, spectroscopy, optical resonators, beam control, atmospheric propagation, laser effects and countermeasures.

Chemistry and Physics Laboratory: Atmospheric chemical reactions, atmospheric optics, light scattering, state-specific chemical reactions and radiative signatures of missile plumes, sensor out-of-field-of-view rejection, applied laser spectroscopy, laser chemistry, laser optoelectronics, solar cell physics, battery electrochemistry, space vacuum and radiation effects on materials, lubrication and surface phenomena, thermionic emission, photosensitive materials and detectors, atomic frequency standards, and environmental chemistry.

Computer Science Laboratory: Program verification, program translation, performance-sensitive system design, distributed architectures for spaceborne computers, fault-tolerant computer systems, artificial intelligence, microelectronics applications, communication protocols, and computer security.

Electronics Research Laboratory: Microelectronics, solid-state device physics, compound semiconductors, radiation hardening; electro-optics, quantum electronics, solid-state lasers, optical propagation and communications; microwave semiconductor devices, microwave/millimeter wave measurements, diagnostics and radiometry, microwave/millimeter wave thermionic devices; atomic time and frequency standards; antennas, rf systems, electromagnetic propagation phenomena, space communication systems.

Materials Sciences Laboratory: Development of new materials: metals, alloys, ceramics, polymers and their composites, and new forms of carbon; nondestructive evaluation, component failure analysis and reliability; fracture mechanics and stress corrosion; analysis and evaluation of materials at cryogenic and elevated temperatures as well as in space and enemy-induced environments.

Space Sciences Laboratory: Magnetospheric, auroral and cosmic ray physics, wave-particle interactions, magnetospheric plasma waves; atmospheric and ionospheric physics, density and composition of the upper atmosphere, remote sensing using atmospheric radiation; solar physics, infrared astronomy, infrared signature analysis; effects of solar activity, magnetic storms and nuclear explosions on the earth's atmosphere, ionosphere and magnetosphere; effects of electromagnetic and particulate radiations on space systems; space instrumentation.